Journal of Enzyme Inhibition and Medicinal Chemistry, April 2006; 21(2): 127–132

Taylor & Francis
Taylor & Francis Group

Quantitative structure–activity relationships (QSARs) in CYP3A4 inhibitors: The importance of lipophilic character and hydrogen bonding

DAVID F.V. LEWIS[1], BRIAN G. LAKE[2] & MAURICE DICKINS[3]

[1]*School of Biomedical and Molecular Sciences, University of Surrey, Guildford, Surrey GU2 7XH, UK,* [2]*BIBRA International Limited, Woodmansterne Road, Carshalton, Surrey SM5 4DS, UK, and* [3]*Pfizer Central Research, Ramsgate Road, Sandwich, Kent CT13 9NJ, UK*

(Received 12 September 2005; in final form 17 November 2005)

Abstract

The results of Quantitative Structure–Activity Relationship (QSAR) analyses on three series of CYP3A4 inhibitors are reported for enzyme inhibition expressed as K_i values. These include a small series of structurally related statins and two larger groupings of structurally diverse compounds, some of which display competitive inhibition of CYP3A4 whereas others act via heme iron ligation. In all cases, however, it is apparent that there are lipophilicity relationships associated with CYP3A4 inhibitory activity in the total of 46 compounds investigated. This is evidenced by linear correlations between inhibition of CYP3A4 and the octanol-water partition coefficient (P value) when expressed logarithmically (ie., log P). In the case of the statins, however, the distribution coefficient (D) at pH 7 is used due to the effect of compound ionization. Conversion of equilibrium constants (ie. K_i and P) to the corresponding free energy changes (ΔG values) facilitates exploration of the likely intermolecular forces of interaction between the inhibitors and the active site region of CYP3A4. In this respect, there appears to be good agreement between QSAR analyses and molecular modelling of the CYP3A4 enzyme itself, and both are consistent with the known mechanisms of inhibition displayed.

Keywords: *CYP3A4, inhibition, partition coefficient, statins, QSAR*

Abbreviations: *K_i, inhibition constant; P, octanol-water partition coefficient; D, distribution coefficient (ionization-corrected partition coefficient); K_m, Michaelis constant; K_D, dissociation constant; IC_{50}, concentration of inhibitor required for 50% inhibition of enzyme activity*

Introduction

The cytochromes P450 (CYP) constitute a superfamily of heme-thiolate enzymes, of which over 4500 individual members are currently known. These play important roles in the metabolism of foreign compounds, and are primarily oxidative in nature [1,2], although reductive metabolism is also known. In addition, there are many P450 enzymes which display endogenous functionality that, in mammalian systems, for example, include: steroid hormone biosynthesis and fatty acid metabolism, together with prostanoid and eicosanoid oxidations [3]. As far as the human drug metabolizing P450s are concerned, it is established that CYP3A4 is involved in the oxidations of a relatively large and structurally-diverse group of chemicals which encompass approximately 30% of all known xenobiotic oxidations [4,5]. Molecular modelling of CYP3A4 based on homology with CYP102 [6] and CYP2C5 [7] has indicated that the majority of CYP3A4 substrates possess a hydrogen bond donor/acceptor atom at a relatively close distance from the preferred site of metabolism, thus providing some rationalization of the likely structural determinants of

Correspondence: D. F. V. Lewis, School of Biomedical and Molecular Sciences, University of Surrey, Guildford, Surrey GU2 7XH, UK. Tel: 441483 686477. Fax: 441483 300803. E-mail: d.lewis@surrey.ac.uk

ISSN 1475-6366 print/ISSN 1475-6374 online © 2006 Taylor & Francis
DOI: 10.1080/14756360500532747

Table I. Statins inhibiting CYP3A4-mediated mexazolam hydroxylation

Compound	$\log D_{7.0}$	K_i (μM)	ΔG_{part}	ΔG_{inh}
1. Pravastatin	2.42	115	−3.4327	−5.5878
2. Simvastatin	4.40	2.13	−6.2413	−8.0450
3. Lovastatin	3.91	2.98	−5.5462	−7.8381
4. Fluvastatin	3.65	7.10	−5.1774	−7.3033
5. Atorvastatin	4.20	2.54	−5.9576	−7.9366
6. Cerivastatin	4.24	2.18	−6.0143	−8.0307
QSAR expressions	n	s	R	F
1. $\Delta G_{inh} = 0.914\ \Delta G_{part} - 2.527$ (± 0.084)	5	0.1847	0.9877	119.71
2. $\Delta G_{inh} = 0.915\ \Delta G_{part} - 2.522$ (± 0.069)	6	0.1600	0.9887	174.00

These statins are all present as the lactone form, apart from Cerivastatin which is likely to exist partially in the acid form also. This has a bearing on the $\log D_{7.0}$ value listed above for Cerivastatin where a weighted average has been taken, based on the reported experimental $\log D_{7.0}$ values [11]. Cerivastatin was omitted from the analysis shown in Equation (1).
n = number of observations; s = standard error; R = correlation coefficient; F = variance ratio.
In the ΔG subscripts, inh refers to inhibition and part refers to partitioning as follows:
$\Delta G_{inh} = RT \ln K_i$ where K_i is the equilibrium constant for inhibition of CYP3A4-mediated activity and $\Delta G_{part} = -RT \ln P$ where P is the octanol–water partition coefficient.
R = gas constant (1.9872 cal $deg^{-1}mol^{-1}$); T = absolute temperature (310K).
Reference to K_i and $\log D_{7.0}$ data: Ishigami et al. 2001 [11].

CYP3A4-substrate selectivity. In addition, several CYP3A4-selective inhibitors, such as ketoconazole at low concentrations, also possess this type of grouping at a similar distance from the heme-ligating imidazole nitrogen than that shown by typical CYP3A4 substrates [6,7]. Furthermore, we have reported previously that lipophilicity relationships exist in CYP3A4 substrates for their binding affinity to the enzyme, on the basis of their K_m or K_D values either towards the expressed enzyme or in human liver microsomes where the involvement of CYP3A4 has been established [8–10].

Table II. CYP3A4 mixed inhibitors⋆

Compound	log P	IC_{50} (μM)	ΔG_{part}	ΔG_{inh}
1. Clotrimazole	5.71[c]	0.002	−8.0994	−12.3392
2. Nicardipine	4.96	0.008	−7.0356	−11.4852
3. Cisapride	3.65[d]	0.038	−5.1774	−10.5253
4. Verapamil	3.79	0.12	−5.3760	−9.8169
5. Cyclosporin	2.92	0.46	−4.1419	−8.9892
6. Midazolam	3.27	0.46	−4.6384	−8.9892
7. Erythromycin	2.48	1.8	−3.5178	−8.1487
8. Astemizole	3.17	0.59	−4.4965	−8.8358
9. Mibefradil	6.22[d]	0.006	−8.8229	−11.6624
10. Nifedipine	2.86	6.6	−4.0568	−7.3483
11. Nimodipine	4.18	0.62	−5.9292	−8.8053
12. Terfenadine	4.00	1.4	−5.6739	−8.3035
13. Troleandomycin	4.26[c]	0.36	−6.0427	−9.1402
14. Ketoconazole	3.73	0.016	−5.2909	−11.9582
QSAR expressions	n	s	R	F
1. $\Delta G_{inh} = 0.927\ \Delta G_{part} - 3.391$ (± 0.074)	5	0.2558	0.991	155.65
2. $\Delta G_{inh} = 0.919\ \Delta G_{part} - 5.012$ (± 0.091)	8	0.3691	0.972	101.00
3. $\Delta G_{inh} = 0.926\ \Delta G_{part} - 4.990$ (± 0.055)	13	0.3047	0.981	279.73
4. $\Delta G_{inh} = 0.924\ \Delta G_{part} - 5.024$ (± 0.055)	14	0.3011	0.980	285.15

c = calculated value (Pallas Software, CompuDrug Limited, Budapest); d = calculated value (ClogP Software, BioByte Corporation, Pomona, California);⋆ = compounds in this dataset exhibit mixed types of inhibition with respect to the mode of inhibition although they would not be regarded as reversible mixed inhibitors in the classical sense.
Reference to IC_{50} data: Ekins et al. 2003 [13].

Table III. Structurally diverse CYP3A4 inhibitors†

Compound	log P	IC_{50} (μM)	ΔG_{part}	ΔG_{inh}	Compound Type
1. Erythromycin	2.54⋆	132	−2.6951	−5.5028	Amine
2. Chloroquine	1.23	350	−1.7447	−4.9021	Amine/quinoline
3. Diltiazem	2.80	217	−3.9717	−5.1966	Amine/diazepine
4. Verapamil	3.79	76	−5.3760	−5.8429	Amine/cyano
5. Bromocriptine	2.37	3	−3.3618	−7.8340	Azole
6. Dihydroergotamine	2.40[c]	3	−3.4043	−7.8340	Azole
7. Troleandomycin	4.16	8	−5.9008	−7.2298	Azole
8. Sulfamethizole	0.54	836	−0.7660	−4.3657	Azole
9. Timoprazole	1.33	309	−1.8866	−4.9789	Azole
10. Piroxicam	1.98	1000	−2.8086	−4.2554	Pyridine
11. Tazanolast	1.39	290	−1.9719	−5.0180	Azole
12. Cimetidine	0.40	1000	−0.5674	−4.2554	Azole
13. Nifedipine	2.86	47	−4.0568	−6.1390	Pyridine
14. Omeprazole	2.23	78	−3.1632	−5.8269	Azole
15. 1-Methylimidazole	−0.06	2700	0.0851	−3.6435	Azole
16. 2-Methylimidazole	0.24	1252	−0.3404	−4.1169	Azole
17. 3-Hydroxypyridine	0.52	768	−0.7376	−4.4180	Pyridine
18. 2-Anilinopyridine	2.75	431	−3.9008	−4.7739	Pyridine
19. AZ-2	3.80	43	−5.3902	−6.1938	Not known
20. Thioperamide	2.41	6.1	−2.5958	−7.3968	Azole
21. Triadimefon	2.77	9.3	−2.7944	−7.1370	Azole
22. Propiconazole	3.50	1.04	−4.4823	−8.4866	Azole
23. Ketoconazole	3.73	0.2	−5.2909	−9.5023	Azole
24. Metyrapone	1.78	4.93	−2.5249	−7.5280	Pyridine
25. Glipizide	1.91	7.44	−2.7093	−7.2745	Pyrazine
26. Miconazole	5.70	0.85	−8.0853	−8.6109	Azole
27. Clotrimazole	5.48	0.05	−7.7732	−10.3563	Azole
28. Fluconazole	0.50	25	−0.7092	−6.5279	Azole
29. Econazole	5.51	0.43	−7.8157	−9.0307	Azole
30. AZ-1	4.00	3.5	−5.6739	−7.7391	Not known

c = calculated value obtained using the Pallas System (CompuDrug Limited, Budapest).

⋆The $\log D_{7.4}$ value is 1.26 for this compound and the ΔG_{part} figure shown above represents an average of the log P and $\log D_{7.4}$ - derived values, thus allowing for the effect of ionization.

†Correlations for this dataset are presented in Table IV and it should be recognized that the mechanisms of inhibition actually differ within the group listed above.

Notes: 1. Econazole and AZ-1 are weak outliers of expression (2), in Table IV; both being about $-0.9\,kcal\,mol^{-1}$ above the line, thus indicating the possible presence of an additional π–π stacking interaction within the CYP3A4 active site. However, they can be included in the dataset satisfactorily with an allowance for the $-0.9\,kcal\,mol^{-1}$ energy difference.

2. Although the inhibitors contain nitrogenous functions which may act as heme ligands, AZ-1 and AZ-2 are AstraZeneca compounds of unknown chemical structure, thus restricting their analysis in terms of potential CYP3A4 active site interactions. However, it is found that AZ-2 conforms well with one of the lipophilicity relationships shown by the other compounds in the group.

Reference to IC_{50} values and some of the experimental log P data: Riley et al. 2001 [14].

Methods

Biological data were taken from the literature for a group of statins, a series of mixed function inhibitors and a larger group of structurally diverse compounds acting as inhibitors of CYP3A4 [11–14]. Lipophilicity data in the form of log P values were also obtained from the literature [15] and, in some cases, calculated using the Pallas System (CompuDrug Limited, Budapest) where the expermentally determined values were unavailable. For the purposes of evaluation of the potential active site interactions with inhibitors, the log P values were converted into their respective ΔG_{part} values using the expression:-

$$\Delta G_{part} = -RT \ln P$$

where R is the gas constant, T is the absolute temperature (taken as 310K) and ln denotes the use of the natural logarithmic function ($\log_e$).

Correlation analyses were performed using the GraphPad software packages InStat and InPlot (GraphPad Software Inc., San Diego, California). The variance ratios (F-test values) were calculated from the correlation coefficients (R values) using the following formula as applied to single regression analyses:

$$F = \frac{R^2(n-3)}{1-R^2}$$

where n is the number of observations (ie. number of data points used in the analysis) associated with the correlation and R is the correlation coefficient.

Table IV. Results of QSAR analysis for three groups of CYP3A4 inhibitors

	n	s	R	F
1. Statins (5 congeners)				
a) $\Delta G_{inh} = 0.914\ \Delta G_{part} - 2.527$ (± 0.084)	5	0.1847	0.988	119.71
b) $\Delta G_{inh} = 0.915\ \Delta G_{part} - 2.522$ (± 0.069)	6	0.1600	0.989	174.00
2. Mixed inhibitors (13 compounds)				
a) $\Delta G_{inh} = 0.901\ \Delta G_{part} - 5.155$ (± 0.093)	7	0.3753	0.974	90.61
b) $\Delta G_{inh} = 0.927\ \Delta G_{part} - 3.391$ (± 0.074)	5	0.2558	0.990	155.65
c) $\Delta G_{inh} = 0.919\ \Delta G_{part} - 5.012$ (± 0.091)	8	0.3691	0.971	101.90
d) $\Delta G_{inh} = 0.926\ \Delta G_{part} - 4.990$ (± 0.055)	13	0.3047	0.980	279.73
e) $\Delta G_{inh} = 0.924\ \Delta G_{part} - 5.024$ (± 0.055)	14	0.3011	0.978	285.15
3. Structurally diverse inhibitors (28 compounds)				
a) $\Delta G_{inh} = 0.590\ \Delta G_{part} - 5.973$ (± 0.045)	9	0.2623	0.979	157.56
b) $\Delta G_{inh} = 0.580\ \Delta G_{part} - 5.894$ (± 0.049)	10	0.2835	0.973	142.73
c) $\Delta G_{inh} = 0.579\ \Delta G_{part} - 3.889$ (± 0.011)	13	0.0873	0.998	304.73
d) $\Delta G_{inh} = 0.694\ \Delta G_{part} - 2.275$ (± 0.095)	5	0.2081	0.973	53.94
e) $\Delta G_{inh} = 0.600\ \Delta G_{part} - 3.827$ (± 0.018)	28	0.2149	0.988	1073.0

n = number of observations; s = standard error; R = correlation coefficient; F = variance ratio.
In the ΔG subscripts, inh refers to inhibition and part refers to partitioning as follows:
$\Delta G_{inh} = RT \ln K_i$ where K_i is the equilibrium constant for inhibition of CYP3A4-mediated activity, $\Delta G_{part} = -RT \ln P$ where P is the octanol-water partition coefficient.
R = gas constant (1.9872 cal $deg^{-1} mol^{-1}$); T = absolute temperature (310K).

With respect to the CYP3A4 inhibition studies, the quantities determined are either IC_{50} or K_i values [12–14,16]. We have converted these into the corresponding free energy changes for inhibition, ΔG_{inh}, according to the following relationship:-

$$\Delta G_{inh} = RT \ln K_i$$

where it is assumed that $K_i \equiv IC_{50}$ for low concentrations of a substrate acting as a competitive inhibitor, thus providing an equivalence between the two types of inhibition data under these conditions. However, the full expression relating K_i, IC_{50} and K_m for different substrate concentrations is provided later, at the end of the following section where its relevance is discussed.

Results and discussion

Tables I–III show the raw data for the three series of compounds, including 5 statins (Table I), 13 CYP3A4 mixed inhibitors (Table II) and 28 structurally diverse CYP3A4 inhibitor (Table III). Table IV presents the results from each set of correlation analyses between ΔG values and ΔG_{part} obtained from octanol-water partition coefficients. Figure 1 shows lipophilicity relationships for the statins, whereas Figures 2 and 3 present similar graphical relationships for the two sets of structurally diverse CYP3A4 inhibitors.

In general, there is similarity between these expressions as all are linear relationships between ΔG_{inh} and ΔG_{part}. Within each group, the equations

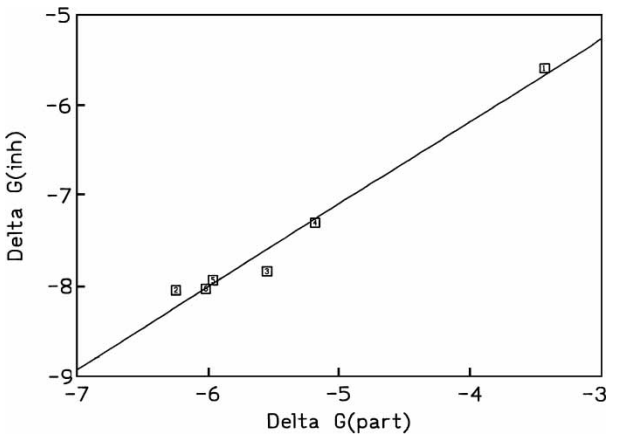

Figure 1. Lipophilicity relationships for a series of statins showing CYP3A4 inhibitory activity. The ΔG_{inh} value is plotted against ΔG_{part} for $\log D_{7.0}$ data and indicates a single hydrogen bond interaction with the CYP3A4 enzyme active site.

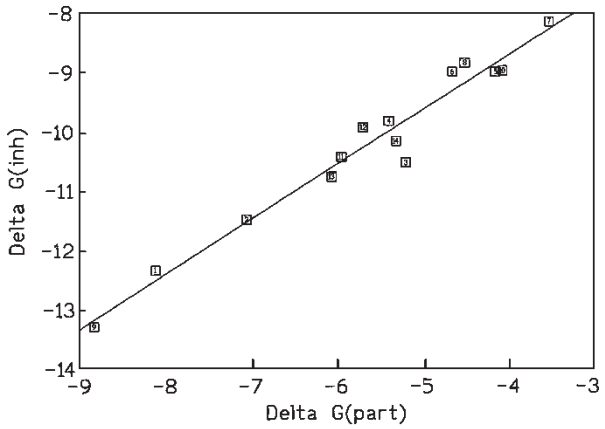

Figure 2. Lipophilicity relationships within a group of 14 structurally diverse CYP3A4 inhibitors. The ΔG_{inh} value is plotted against ΔG_{part} for log P data and indicates that the difference between the two lines is equivalent to an average hydrogen bond energy of -1.5 kcal mol^{-1}.

show roughly the same gradient, by and large, although there is a marked variation between the three series of compounds. The reason for this is not clear but may relate to differences in mechanism of inhibition or possibly due to differences between regions of the CYP3A4 active site where a molecule may bind, although the former, may only affect the values of the intercepts shown in these equations rather than their gradients.

For the small group of statins, the slopes produced are close to those obtained for the larger set of mixed inhibitors, being around 0.91 in value. In the case of Equation (2e) in Table IV, this represents all 14 compounds in the dataset by compensating for the different intercepts shown in Equations (2b) and (2c), which roughly approximates to -2 kcal mol^{-1}, and this is probably due to an additional hydrogen-bonded interaction for the compounds involved in Equation (2c) (Table IV). Clearly the intercept in Equation (2d) is close to that of Equation (2c), thus providing some degree of confidence in the approach used. A similar situation is shown by the group of 28 structurally diverse compounds in the third series, with Equations (3a)–(3e) in Table IV.

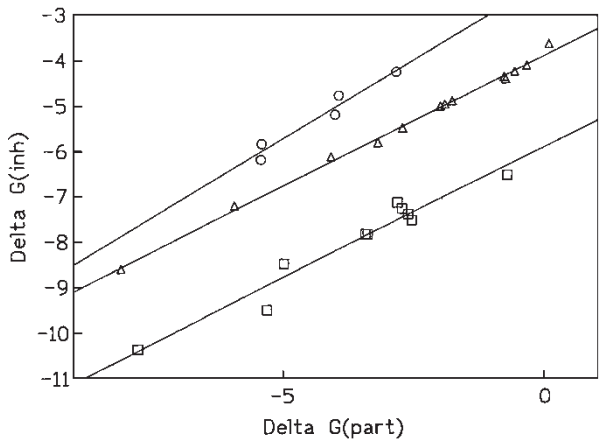

Figure 3. Lipophilicity relationships within a group of 28 structurally diverse CYP3A4 inhibitors. The ΔG_{inh} value is plotted against ΔG_{part} for log P data and indicates that the difference between two of the lines is equivalent to an average hydrogen bond energy of -1.6 kcal mol^{-1}. However, the difference between the two upper lines is equivalent to an average hydrogen bond energy of -2 kcal mol^{-1}.

The slopes are very similar for the different expressions and the changes in intercepts reflect the likely variations in hydrogen-bonded interactions formed by the various subsets. Consequently, it has been possible to combine the individual subseries of compounds, exemplified by Equations (3b), (3c) and (3d), into a single expression for all 28 congeners to produce a very good correlation ($R = 0.988$) between the inhibition and partition free energies (shown as Equation (3e), Table IV). It would appear that hydrogen bonding is of importance for substrates and inhibitors binding to CYP3A4, based on recent evidence from the crystal structure. Furthermore, the potential for extensive π-π stacking interactions also exists due to the presence of a cluster of at least five aromatic residues in the vicinity of the active site [17,18]. It is generally accepted that the local dielectric constant varies from a value of about 4 at the interior of globular proteins to around 36 at the surface, as opposed to the experimental value of 78 for the dielectric constant of bulk water. However, an alternative explanation may lie in the different methodologies used for the inhibition measurements and, of course, in the relationship between K_i and IC_{50}, as shown in [14], where:

$$K_i = \frac{IC_{50}}{1 + ([S]/K_m)}$$

such that $K_i \cong IC_{50}/2$ when the substrate concentration [S] is approximately equal to the K_m value [19]. Although, we do not have information on the K_m data, this factor of 2 would give rise to a difference in the corresponding ΔG_{inh} values for K_i and IC_{50} determinations which may, in part, explain the differences in slopes for the lipophilicity relationships described. For low substrate concentrations, however, it can be appreciated, by inspection of the above equation, that $K_i \cong IC_{50}$ (because the denominator is approximately unity) as mentioned previously in the Methods section. These differences could therefore help to explain the variations in the graphical plots observed between the different series of CYP3A4 inhibitors. However, this situation occurs for the set of structurally diverse CYP3A4 inhibitors only, and the slopes for the two other series are extremely close in value, lying between 0.9 and 0.926 according to the

equations presented in Table IV for the first and second series of compounds.

Conclusions

The inhibition of CYP3A4 in the three series of compounds investigated is correlated closely with their lipophilic character in the form of log P, where P is the octanol-water partition coefficient or by $\log D_{7.4}$, which is the logarithm of the distribution coefficient at pH 7.4. The linear lipophilicity relationships indicate that desolvation of the active site is the primary contributing factor to inhibition of the CYP3A4 enzyme, irrespective of the structural class of compound. Furthermore, hydrogen bonding represents a common interaction between the inhibitors and at least one active site hydrogen bond donor/acceptor amino acid residue, and serine-119 constitutes a most likely candidate for this interaction as it is thought to reside close to the heme iron [20]. The homology modelling of CYP3A4 [7] shows that compounds possessing a hydrogen bond donor/acceptor atom at an optimal distance from the position of metabolism (or inhibition for heme ligands) are probably selective for CYP3A4 and this is supported by molecular modelling of a substrate template with the CYP3A4 crystal structure, where serine-119 makes a hydrogen-bonded contact with each substrate investigated thus far. The appearance of different gradients for the lipophilicity relationships may indicate different modes (and corresponding dielectric constants) of binding to the CYP3A4 active site, being associated with allosteric behaviour [21] where it is possible that several binding sites exist for different types of compound [13,18].

Acknowledgements

The financial support of GlaxoSmithKline Research and Development Limited, Merck, Sharp & Dohme Limited and the University of Surrey Foundation Fund is gratefully acknowledged by one of us (DFVL).

References

[1] Lewis DFV. Cytochromes P450: Structure, function and mechanism. London: Taylor & Francis; 1996.
[2] Lewis DFV. Guide to cytochromes P450 structure and function. London: Taylor & Francis; 2001.
[3] Lewis DFV. 57 varieties: The human cytochromes P450. Pharmacogenomics 2004;5:305–318.
[4] Rendic S, DiCarlo FJ. Human cytochrome P450 enzymes: A status report summarizing their reactions, substrate, inducers and inhibitors. Drug Met Rev 1997;29:413–580.
[5] Rendic S. Summary of information on human CYP enzymes: Human P450 metabolism data. Drug Met Rev 2002; 34:83–448.
[6] Lewis DFV, Eddershaw PJ, Goldfarb PS, Tarbit MH. Molecular modelling of CYP3A4 from an alignment with CYP102: Identification of key interactions between putative active site residues and CYP3A-specific chemicals. Xenobiotica 1996;6:1067–1086.
[7] Lewis DFV, Lake BG, Dickins M, Goldfarb PS. Homology modelling of CYP3A4 from the CYP2C5 crystallographic template: Analysis of typical CYP3A4 substrate interactions. Xenobiotica 2004;34:549–569.
[8] Lewis DFV. Quantitative Structure–Activity relationships (QSARs) for substrates of human cytochromes P450 CYP2 family enzymes. Tox in Vitro 2004;18:89–97.
[9] Lewis DFV, Jacobs MN, Dickins M. The importance of compound lipophilicity for substrate binding to human P450s involved in drug metabolism. DDT 2004;9:530–537.
[10] Lewis DFV, Dickins M. Baseline lipophilicity relationships in human cytochromes P450 associated with drug metabolism. Drug Met Rev 2003;35:1–18.
[11] Ishigami M, Honda T, Takasaki W, Ikeda T, Komai T, Ito K, Sugiyama Y. A comparison of the effects of 3-hydroxy-3-methylgutaryl-coenzyme A (HMG-CoA) reductase inhibitors on the CYP3A4-dependent oxidation of mexazolam *in vitro*. Drug Met Disp 2001;29:282–288.
[12] Stresser DM, Blanchard AP, Turner SD, Erve JCL, Dandeneau AA, Miller VP, Crespi CL. Substrate-dependent modulation of CYP3A4 catalytic activity: analysis of 27 test compounds with four fluorometric substrates. Drug Met Disp 2000;28:1440–1448.
[13] Ekins S, Stresser DM, Williams JA. In vitro and pharmacophore insights into CYP3A enzymes. TIPS 2003;24:161–166.
[14] Riley RJ, Parker AJ, Trigg S, Manners CN. Development of generalized, quantitative physicochemical model of CYP3A4 inhibition for use in early drug discovery. Pharm Res 2001;18:652–655.
[15] Hansch C, Leo A, Hoekman D. Exploring QSAR: hydrophobic electronic and steric constants. Am Chem Soc 1995.
[16] Ekins S, Bravi G, Binkley S, Gillespie JS, Ring BJ, Wikel JH, Wrighton SA. Three-dimensional quantitative Structure–Activity relationship (3D-QSAR) analysis of inhibitors of CYP3A4. J Pharm Exp Ther 1999;290:429–438.
[17] Yano JK, Wester MR, Schoch GA, Giffin KJ, Stout CD, Johnson EF. The structure of human microsomal cytochrome P450 3A4 determined by X-ray crystallography to 2.05Å resolution. J Biol Chem 2004;279:38091–38094.
[18] Williams PA, Cosme J, Vinkovic DM, Ward A, Angove HC, Day PJ, Vonrhein C, Tickle IJ, Jhoti H. Crystal structures of human cytochrome P450 3A4 bound to metyrapone and progesterone. Science 2004;305:683–686.
[19] Cortes A, Cascante M, Cardenas ML, Cornish-Bowden A. Relationships between inhibition constants, inhibitor concentrations for 50% inhibition and types of inhibition: New ways of analyzing data. Biochem J 2001;357:263–268.
[20] Domanski TL, Halpert JR. Analysis of mammalian cytochrome P450 structure and function by site-directed mutagenesis. Curr Drug Met 2001;2:117–137.
[21] Atkins WM. Implications of the allosteric kinetics of cytochrome P450s. DDT 2004;9:478–484.